Pal et al. | Article 8413
J Pure Appl Microbiol. 2023;17(2):919-930. doi: 10.22207/JPAM.17.2.20
Received: 08 January 2023 | Accepted: 01 February 2023
Published Online: 04 May 2023

P-ISSN: 0973-7510; E-ISSN: 2581-690X

RESEARCH ARTICLE OPEN ACCESS

COVID-19 Prognosis from Chest X-ray Images by using Deep Learning Approaches: A Next Generation Diagnostic Tool

Madhumita Pal[1,2], Smita Parija[1]*, Ganapati Panda[1], Snehasish Mishra[3], Ranjan K. Mohapatra[4]* and Kuldeep Dhama[5]

[1]Department of Electronics and communication Engineering, CV Raman Global University, Bidyanagar, Mahura, Janla, Bhubaneswar, Odisha, India.
[2]Department of Electrical Engineering, Government College of Engineering, Keonjhar, Odisha, India.
[3]School of Biotechnology, Campus-11, KIIT Deemed University, Bhubaneswar, Odisha, India.
[4]Department of Chemistry, Government College of Engineering, Keonjhar, Odisha, India.
[5]Division of Pathology, ICAR-Indian Veterinary Research Institute, Izatnagar, Bareilly, Uttar Pradesh, India.

Abstract

Global public health is overwhelmed due to the ongoing Corona Virus Disease (COVID-19). As of October 2022, the causative virus SARS-CoV-2 and its multiple variants have infected more than 600 million confirmed cases and nearly 6.5 million fatalities globally. The main objective of this reported study is to understand the COVID-19 infection better from the chest X-ray (CXR) image database of COVID-19 cases from the dataset of CXR of normal, pneumonia and COVID-19 patients. Deep learning approaches like VGG-16 and LSTM models were used to classify images as normal, pneumonia and COVID-19 impacted by extracting the features. It has been observed during the COVID-19 pandemic peaks that large number of patients could not avail medical beds and were seen stranded outdoors. To address such health emergency situations with limited available bed and scarcity of expert physicians, computer-aided analysis could save precious lives through early screening and appropriate care. Such computer-based deep-learning strategy could help during future pandemics, especially when the available health resources and the need for preventive measures to take do not match the burden of a disease.

Keywords: COVID-19 Prognosis, X-ray Image, Deep Learning, Long Short-term Memory (LSTM), VGG 16

***Correspondence:** ranjank_mohapatra@yahoo.com; smita.parija@gmail.com

Citation: Pal M, Parija S, Panda G, Mishra S, Mohapatra RK, Dhama K. COVID-19 Prognosis from Chest X-ray Images by using Deep Learning Approaches: A Next Generation Diagnostic Tool. *J Pure Appl Microbiol.* 2023;17(2):919-930. doi: 10.22207/JPAM.17.2.20

INTRODUCTION

The continuously emerging and reemerging SARS-CoV-2 variants have led to a huge health crisis worldwide. Besides health crisis, the pandemic has significantly affected global economy.[1] The pathogen grappled the globe with multiple waves after originating from Wuhan, China, in the late 2019.[1-4] This pandemic highly transmissible virus in its multiple mutated variant forms has killed millions globally, mainly due to human-human transmission.[5] Initially, the Delta variant was most deadly and later the Omicron variant and its sub-lineages prevailed as the most infective ones. Emerging sub-lineages like BA.1, BA.2, BA.3, BA.4/5, BA.2.75, BA.4.6 tremendously affected healthcare infrastructure at global-scale. The virus reportedly gradually infected the upper and lower respiratory system, heart, kidney, liver, gut and the nervous system, leading to multiorgan damage.[6,7] It also causes severe health issues in the immunocompromised or comorbid with diabetes, obesity, cardiovascular disorder, psychiatric disorder, etc.[8-10]

The currently circulating highly transmissible and immunity-evasive subvariants like XBB, BF.7, BQ.1and BQ.1.1.[11-14] To contain the virus, numerous measures were implemented. However, its continuously emerging mutating multiple virus variants have tremendously affected global healthcare infrastructure. Another major challenge that surfaced is the shortage of test kits and similar medical gadgets. Also, the seemingly low safety and efficacy of the available COVID-19 vaccines also play a crucial role in the emergence of virus variants.[15,16] The pandemic continues to threaten the global population as a result. In such a scenario, early and automatic screening of samples may improve healthcare facility worldwide to handle the extraordinary health crisis. Various AI-based (especially ML and DL) techniques have been tried previously, for automatic screening of COVID-19 cases.[17]

Zhang et al.[18] developed CNN architecture for early automatic diagnosis of COVID-19 cases. They proposed the CNN-based approach for prognosis by utilising three different views of the CXR image (left lung, right lung and overall view) to extract individual features. The proposed model is effective for binary classification of healthy and COVID-19 cases. Haque and Abdelgawad[19] reported a custom convolutional neural network model to detect COVID-19 with 98.3% accuracy. A major issue of this model is, it cannot differentiate COVID-19 cases from other non-COVID cases (like pneumonia). Ghoshal and Tucker[20] applied a Bayesian convolutional neural network (BCNN) on publicly available COVID-19 CXR images. Results demonstrated an improved (85.2–92.9%) detection accuracy using VGG-16 model. Islam et al.[21] proposed DL technique to automatically detect COVID-19 from CXR images by combining CNN and LSTM. This model achieved 99.4% accuracy with high degree of sensitivity and specificity. Narin et al.[22] used InceptionV3, ResNet50 and InceptionResNetV2 models to categorise CXR images into COVID-19 and normal. With the small dataset for binary classification, they achieved highest accuracy (98%) using ResNet50. Shorfuzzaman et al.[23] proposed a novel CNN based DL fusion framework using transfer learning concept to detect COVID-19 from CXR images with 95.49% classification accuracy. The performance of the proposed models was assessed with CXR image dataset of the healthy, COVID-19 and the pneumonia infected. This research work presents two deep learning approaches using CXR images for early automatic prognosis of COVID-19.

MATERIALS AND METHODS

Methodology

The COVID-19 CXR image dataset was used to perform COVID-19 prognosis. Dataset used for the work was sourced from https://github.com/ieee8023/covid-chestxray-dataset.[24] It contained 5863 images collected from hospitals, public sources and directly from physicians. It had 94 normal CXR images, 506 of COVID-19 and 46 of pneumonia. Two deep learning models, VGG16 and LSTM, were implemented to study the normal, COVID and pneumonia cases from the images. The study plan is schematically presented in Figure 1. The COVID-19 CXR image database was considered first. Then the features from the images were extracted. Then, deep learning models with 200 epochs were implemented on the database. 80% data were considered for training and 20%

data for the run. The performance accuracy, the ROC (receiver operating characteristics curve), precision, recall and F1 score of each model were ascertained. SoftMax classifier was used to classify images into normal, COVID-19 and pneumonia.

Dataset

As indicated, the dataset for the study was accessed from the publicly available resources (at https://github.com/ieee8023/covid-chestxray-dataset). Dataset was processed in Python open-source software. TensorFlow environment was used to process. Keras, Pandas, NumPy, and matplotlib packages were used. The data were contained in two folders, one to train and the other for test, and both train and test folders contained three subfolders (normal, COVID-19 and pneumonia; In Figure 2, the normal CXR image depicted clear lungs without any abnormal opacity, COVID-19 image exhibited a focal lobar consolidation, and pneumonia image had a more diffuse interstitial pattern in both the lungs. The dataset contained 6432 X-ray images in all and 20% of the images were considered as test data. All CXR images were curated for consistency and quality by removing all low quality or unreadable

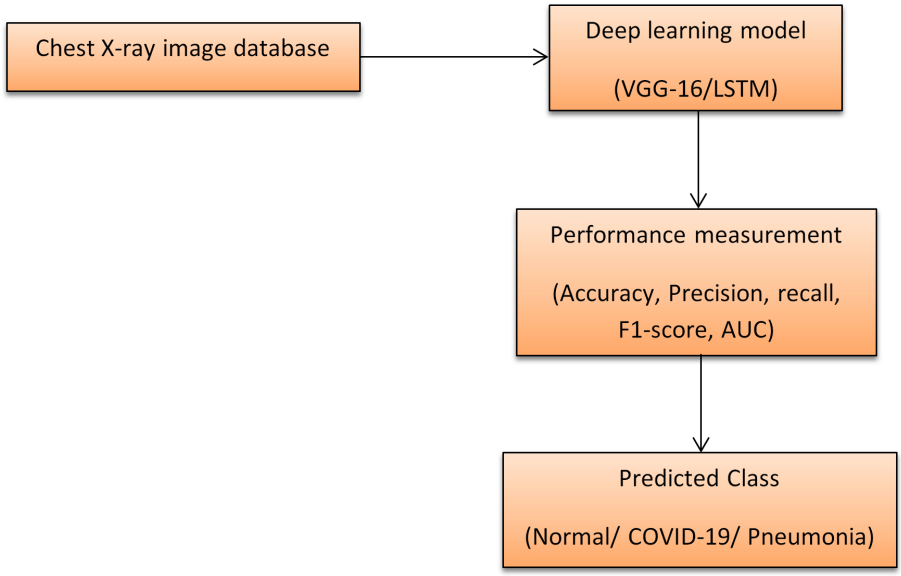

Figure 1. CXR images classification for diagnosis-based COVID-19 transmission probability

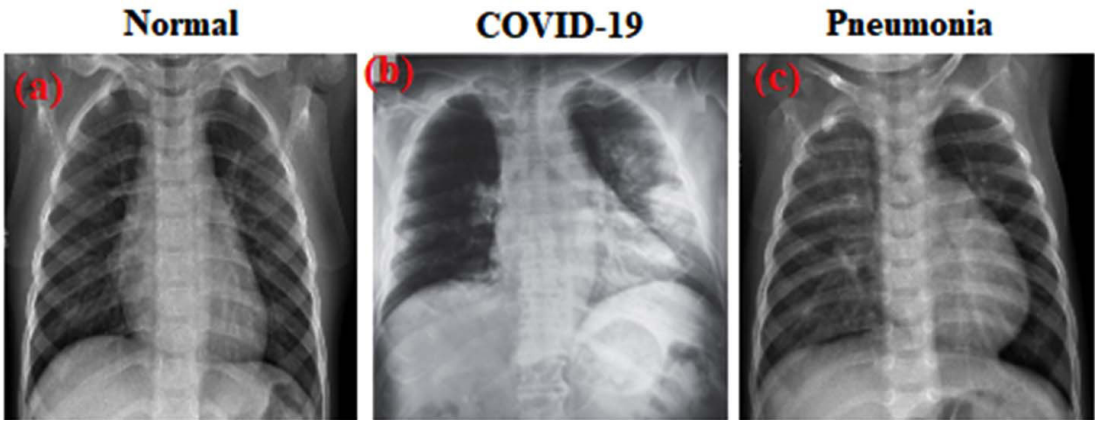

Figure 2. Sample CXR images from curated dataset: a) normal; b) COVID-19; c) pneumonia

scans before clearing for training the AI system.
No. of training images of Normal CXR: 1266
No. of training images of COVID CXR: 460
No. of training images of pneumonia CXR: 3418
Total: 5144
No. of test images of Normal CXR: 317
No. of test images of COVID CXR: 116
No. of test images of pneumonia CXR: 855
Number of test images: 1288

Data preprocessing

Image preprocessing and augmentation API of Keras (known as ImageDataGenerator) was used during the training. Following operations were performed by the API on the data:
Rescaling: Performed for min-max scaling for pixels of each channel.
Rotation: Images were rotated within -10 to +10° range.
Lateral shift (width shift): Images were shifted laterally in either direction by 10%.
Vertical shift (height shift): Images were shifted vertically in top-down direction by 10%.
Horizontal flip: Mirrored image of the original X-ray scan were taken across the vertical axis.

The Rectified Linear Unit activation function triggered activation of each hidden layer. The form of the input image was [224, 224, 3].

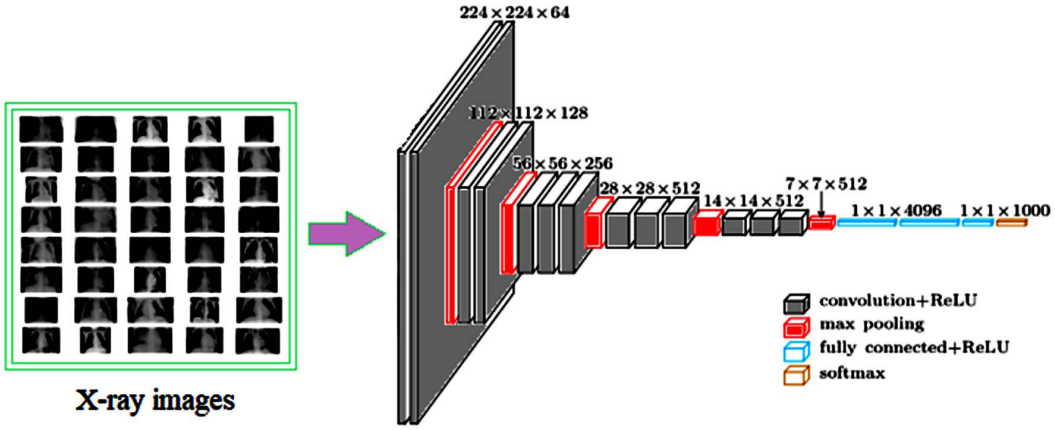

Figure 3. Structure of VGG16 model (created with Image online.co; ref. 25)

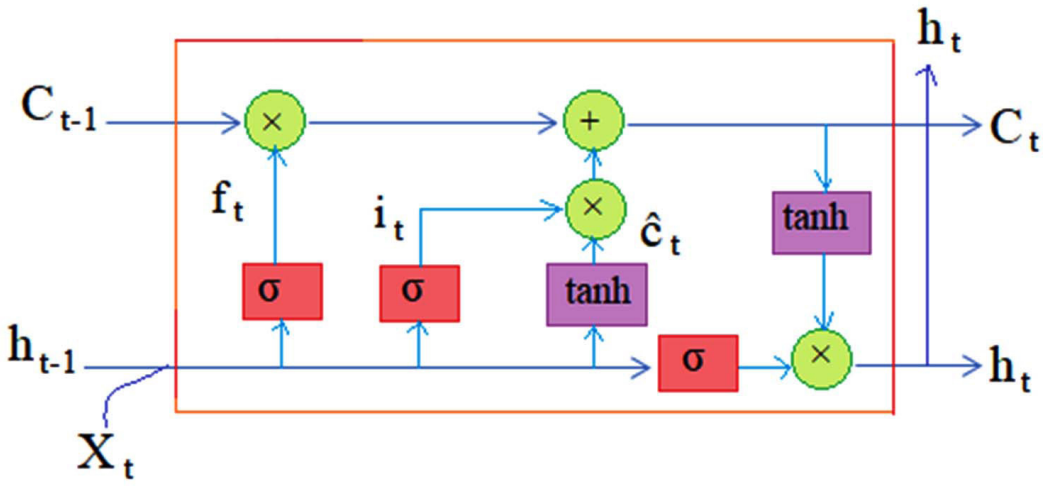

Figure 4. Block diagram for LSTM architecture (tanh lied between -1 and 1; σ between 0 and 1)

Each model was trained for 200 epochs. The batch size was 32, the learning rate was set to 0.0001, and ADAM was used as the loss function. It was decided to train a cross-entropy loss function on all models.

VGG16

VGG16 (Figure 3) is an advanced version of CNN architecture with distinct feature. The architecture consists of convolutional layer, pooling layer and two fully connected layer. The last layer of the architecture is soft max classifier. It has less number of hyper parameters. Relu activation function is used for triggering the hidden layer units of CNN. The convolution and max pool layers are arranged in same fashion throughout the architecture. VGG16 contains differentially weighed 16 layers, a huge network with 138 million trainable parameters.

Total parameters: 134,272,835
Trainable parameters: 134,272,835
Non-trainable parameters: 0
{'COVID-19': 0, 'NORMAL': 1, 'PNEUMONIA': 2}

Long short-term memory (LSTM)

Long short-term memory (LSTM) is a DL (RNN) architecture developed by Hochreiter and Schmidhuber.[26] LSTM has the ability to handle total data points instead of single data points. It contains memory elements and consists of input gate, forget gate and output gate which control the flow of information through LSTM architecture. LSTMs is a type of RNN used for eliminating the long term dependency problem and can remember information for longer duration due to its feedback connection.[27] Sigmoid gate is known as forget gate which helps in selection of data passing though LSTM architecture. The sigmoid function forms the input layer which takes the output of the last LSTM unit (ht1) at time t=1 and the current input (x_t) at time t, which determines the process of detecting and excluding data. The sigmoid function also determines which aspect of the earlier output could be removed. Tanh layer is an added new vector (ĉ) to update state value. h_{t-1} and x_t form the forget gate (Figure 4) and returns 0 and 1 as the value, 1 representing storing the information and 0 representing removing the information from the cell.

The output of forget gate from Figure 2 is:

$$f_t = \sigma(W_f.[h_{t-1}X_t] + b_f) \quad ...(1)$$

$$i_t = (W_t.[h_{t-1},X_t]+b_t \quad ...(2)$$

$$\hat{c}_t = tanh\ (W_c.\ [h_{t-1},X_t] + b_c \quad ...(3)$$

$$C_t = f_t\ X\ C_{t-1} + i_t\ X\ _Ct \quad ...(4)$$

$$O_t = (W_0.[h_{t-1}, X_t]+b_o) \quad ...(5)$$

$$h_t = O_t\ X\ tanh(C_t) \quad ...(6)$$

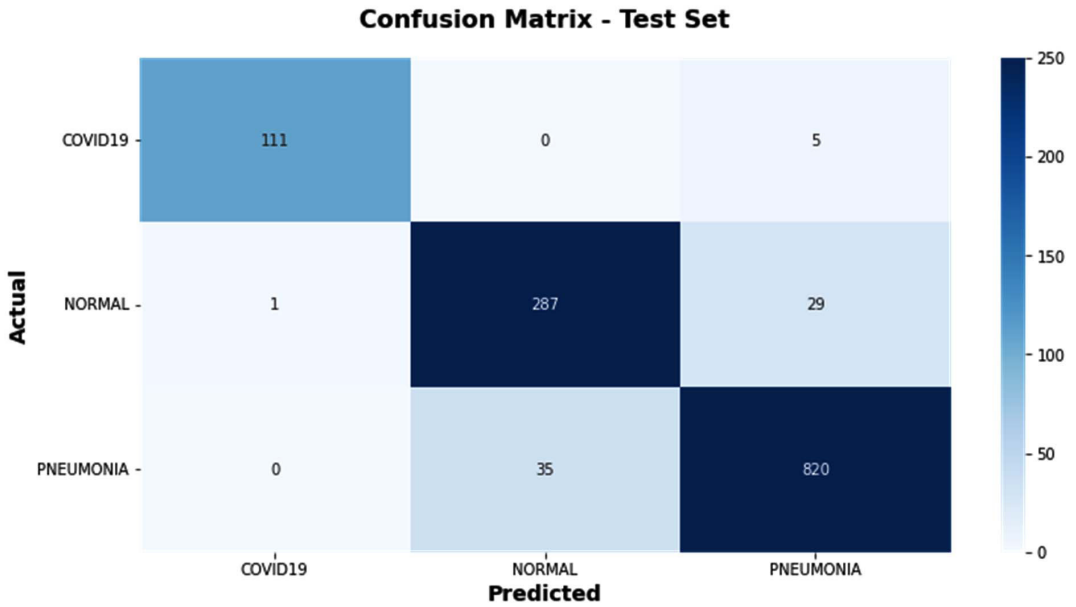

Figure 5. Confusion matrix of LSTM model

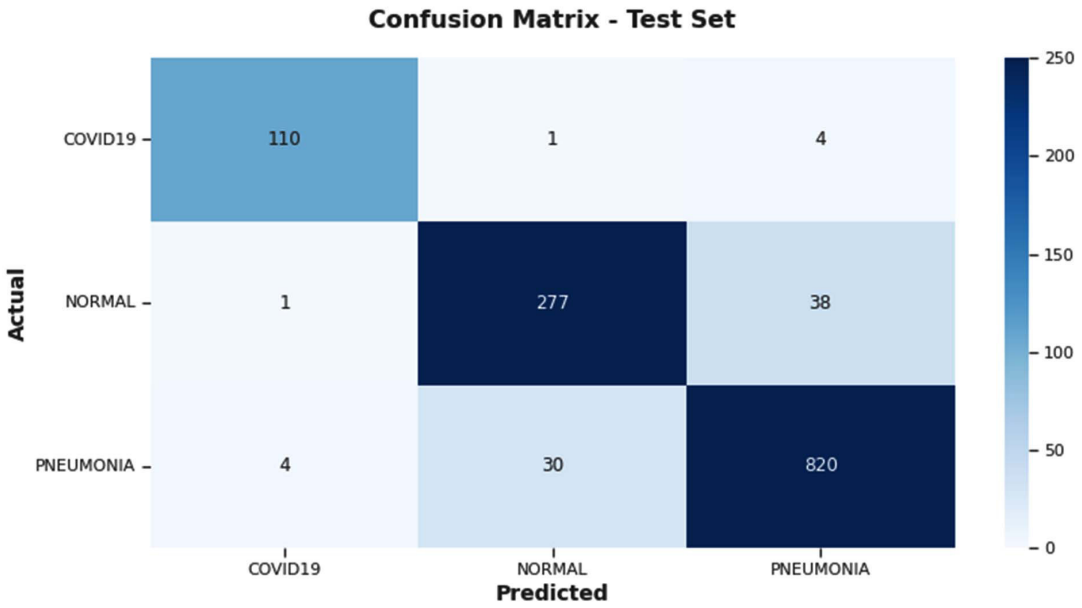

Figure 6. Confusion matrix of VGG16 model

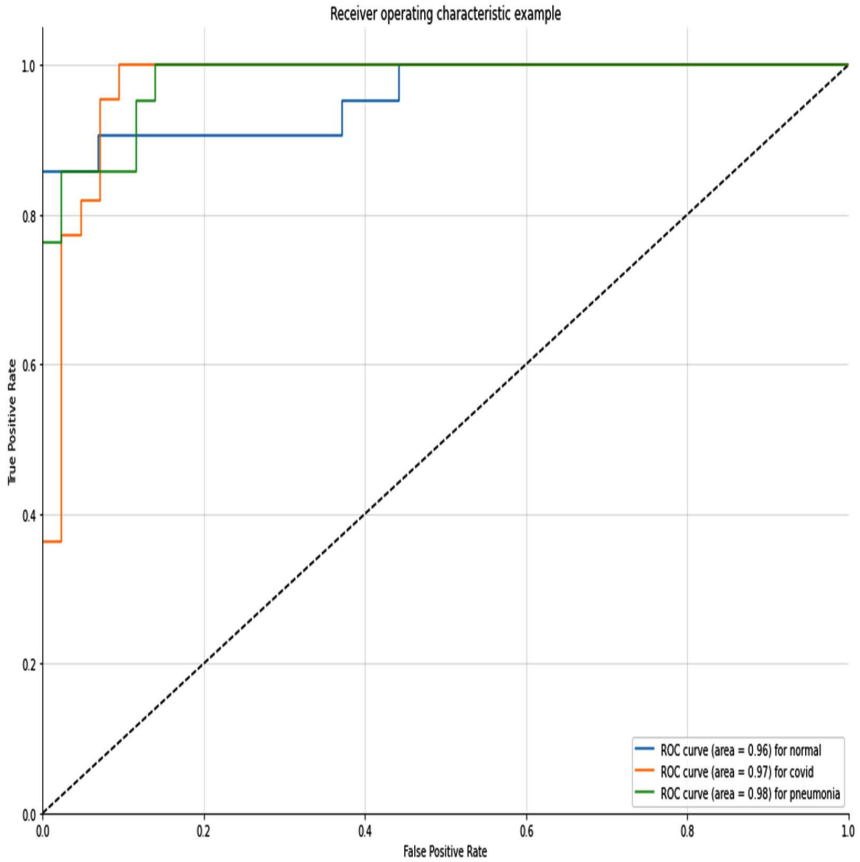

Figure 7. ROC curve of LSTM model

where, C_{t-1} = old cell state, C_t = new cell state, σ = sigmoid layer, tanh = tan hyperbolic layer

RESULTS AND DISCUSSION

CXR image database accessed from the GitHub site containing three groups of RGB images, normal CXR, COVID CXR and Pneumonia CXR was used for the study. LSTM and VGG16 models were implemented to classify the images. The performance of each model in terms of confusion matrix, receiver operating characteristics curve (ROC), training and validation accuracy loss curve are explained below.

Performance measure in terms of confusion matrix

The confusion matrix of each model was assessed (Table 1 and 2). It is a matrix that measures the ability of a deep learning model to classify images (as normal, COVID-19, and pneumonia in this case). Being a three-class problem a 3*3 confusion matrix where the first cell represented the true positive samples was implemented. The confusion matrix contained four parameters as True Positive (TP), True Negative (TN), False Positive (FP) and False Negative (FN) as detailed below:

Table 1. Confusion matrix report of LSTM model

X-Ray image type	TP	FN	FP	TN
COVID-19	111	05	01	1171
Normal	287	30	35	936
Pneumonia	820	35	34	399

Table 2. Confusion matrix report of VGG16 model

Types of X-ray image	TP	FN	FP	TN
COVID-19	110	05	05	1165
Normal	277	39	31	938
Pneumonia	820	34	42	389

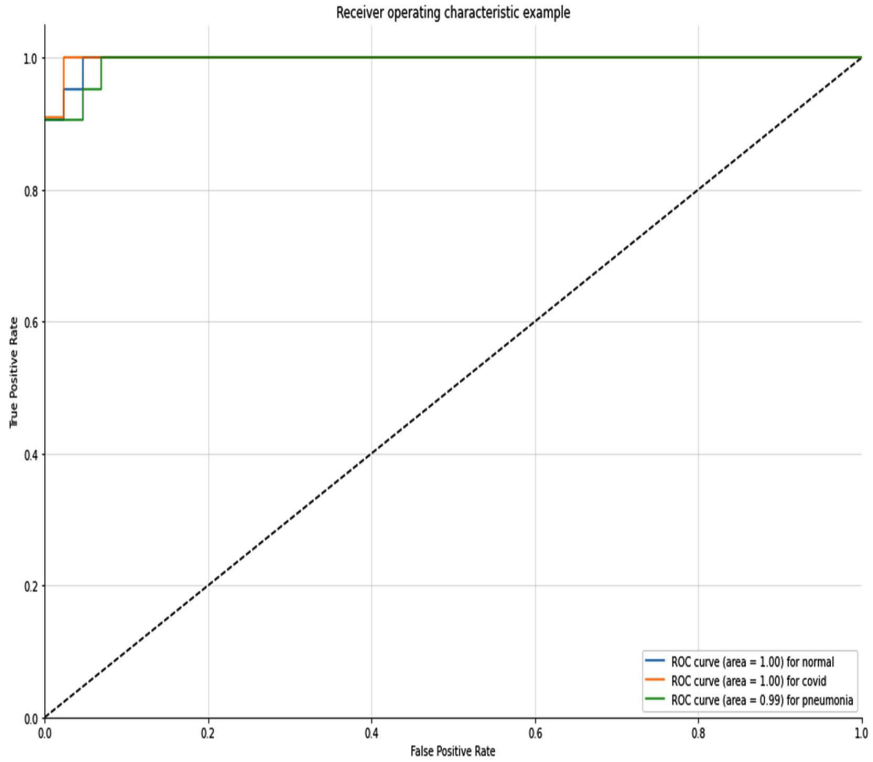

Figure 8. ROC of VGG16 model

TP

A true positive value had the actual and anticipated values as same. It represented the actual number of disease cases.

FN

Cells 2 and 3 represented false negative values. The FN value was the sum of the values of corresponding rows except the TP value. It accounted for all COVID-19 and pneumonia positive cases that were misdiagnosed as negative cases.

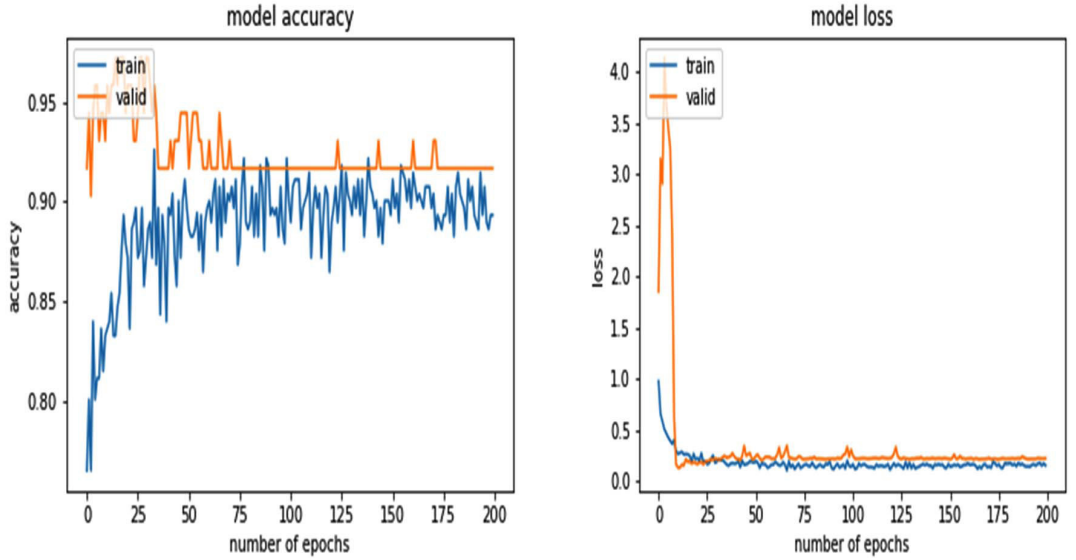

Figure 9. Accuracy and loss curve of LSTM model

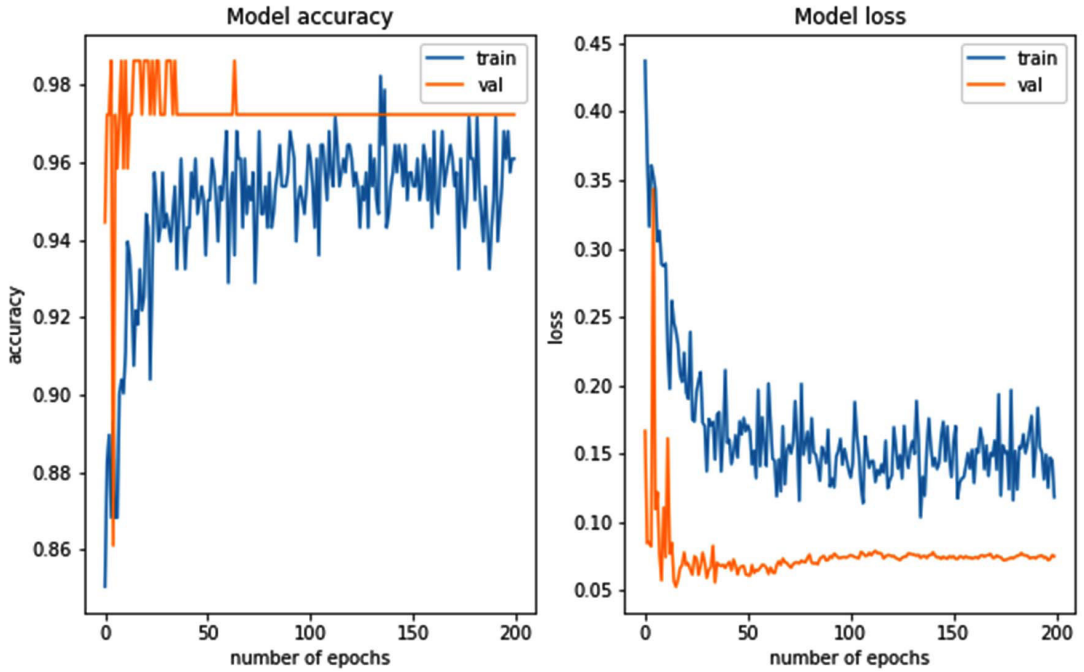

Figure 10. Accuracy and loss curve of VGG16 model

Table 3. Performance parameter values of deep learning models

Deep learning model	Chest X-ray type	Precision	recall	F1 score
VGG16	Normal	0.96	0.96	0.96
	COVID	0.90	0.88	0.89
	Pneumonia	0.95	0.96	0.96
LSTM	Normal	0.99	0.96	0.97
	COVID	0.89	0.91	0.90
	Pneumonia	0.96	0.96	0.96

FP

The false positive value was the sum of the values of the corresponding column except the TP value. It accounted for all COVID-19 and pneumonia negative cases misdiagnosed as positive cases.

TN

The true negative value was the sum of all columns and rows excluding the values of the class for which the values were being calculated. It indicated the number of healthy patients that were actually not suffering from either COVID-19 or pneumonia.

The confusion matrices of each model are presented in Figure 5 and 6.

Model performance in terms of ROC curve

The graph between true positive (TP) and false positive (FP) rates showed the ability of deep learning models to classify. More the area covered by the curve more shall be the accuracy of the prognosis by a model. ROC curves of each model are shown in Figure 7 and 8. VGG16 model performed better than LSTM in prognosing COVID-19 and pneumonia patients with a ROC value of 100% and 99%, respectively (Figure 8). LSTM model prognosed COVID-19, pneumonia and normal patients with 97%, 98% and 96% ROC values, respectively. The performance metrics formulae of DL models are as bellow:

$$\text{Precision (P)} = \frac{TP}{TP + FP}$$

$$\text{Recall or TP, R} = \frac{TP}{TP + FN}$$

$$\text{F1- score} = 2 \text{ X } \frac{P \text{ X } R}{P + R}$$

$$\text{FPR} = \frac{FP}{FP + TN}$$

Performance of models in terms of precision, recall and F1 score

Performance parameters of the models for the image database are provided in Table 3. The precision, recall and F1 score for VGG16 and LSTM models were obtained from Table 3. VGG16 returned reliable precision (0.95), recall (0.95) and F1 score (0.95) values for COVID-19 prognosis. For normal classification, the values obtained were precision: 0.91, recall: 0.95 and F1 score: 0.93. For pneumonia prognosis, the values obtained were precision: 0.95, recall: 0.90 and F1 score: 0.93. Compared to VGG16 the performance of LSTM model on precision (0.86), recall (0.82) and F1 score (0.84) in COVID-19 prognosis was relatively low, and the model returned precision, recall and F1 score values of 0.95, 0.86 and 0.90 respectively for normal classification. The performance of LSTM model for pneumonia classification was precision: 0.79, recall: 0.90 and F1 score: 0.84 values, respectively. High recall value indicated lower false negative prognosis values. False negative prognosis may misdiagnose a patient. Among the two test models, VGG16 was suitable for correct COVID and pneumonia prognosis as it exhibited higher recall value.

Model performance in terms of training and validation curve

LSTM model provided 92% validation accuracy and 88% training accuracy after 200 epochs (Figure 9). Validation loss of 0.01 and training loss of 0.001 were obtained at 11 epochs. After 11 epochs validation accuracy was superior to the training accuracy. Validation accuracy was at its maximum value at 35 epochs. At 200 epochs, 0.2 validation loss and 0.1 training loss were obtained.

VGG16 model returned best performance compared to LSTM model (Figure 10). The training accuracy showed better performance than validation accuracy initially for VGG16 model.

Table 4. Deep learning methods and techniques used in COVID-19 using CXR images

Study	Architecture	Accuracy (%)	References
Apostolopoulos et al.	VGG-19	93.48%	28
Narin et al.	InceptionV3	97	22
Sahinbas and Catak,	VGG-16, VGG-19, ResNet, DenseNet, InceptionV3	80	29
Guefrechi et al.	Resnet50	97.20	30
Jamil and Hussain	Deep CNN	93	31
Joaquin	ResNet-50	96.2	32
Brunese et al.	VGG-16	96	33
Rajaraman and Antani,	VGG16	93	34
Proposed model	LSTM	92	-
	VGG16	97	-

Validation accuracy improved after 11 epochs as compared to training accuracy. It performed superior to training accuracy with 100% accuracy at 71 epochs and after that it remained constant. Validation accuracy remained constant at 97% with a loss of 0.05 after 71 epochs, whereas training accuracy maximised to 98.94% at 145 epochs. A validation loss of 0.05 with 11 epochs and a training loss of 0.12 after 145 epochs were observed. A validation accuracy of 0.97 and a loss of 0.07, and training accuracy of 0.95 and a loss of 0.13 were obtained at 200 epochs.

Comparative analysis

The performance and reliability of the proposed systems were compared with the state-of-art COVID-19 probing systems. Outcome of the first version of the proposed system is presented and compared with conventional methods in Table 4. The proposed system demonstrated remarkably accurate results compared to conventional methods. Also, the proposed improved Resnet-50 system is lightweight as compared to models like VGG16 or DenseNet. The proposed system outperformed the existing methods on precision, accuracy, sensitivity and F1 score. Table 4 lists the findings of the auto-prognosis of COVID-19 using CXR images which was contrasted with the suggested model. Narin et al.[22] used 26 million parameters for COVID-19 prognosis, the two improved models outperformed other models in terms of accuracy (Table 4). Proposed VGG16 model used roughly five times as many (134 million parameters). This model costs more while is marginally higher on accuracy (97.5%) compared to other models.

CONCLUSION

This paper demonstrates application of VGG16 and LSTM deep learning techniques to CXR images for COVID-19 prognosis, using public repository dataset for multi-class and binary classification tasks. The LSTM model provided 98% validation accuracy and 92% training accuracy while the respective figures were 100% and 98.94% for VGG16. The validation loss of 0.01 and training loss of 0.001 were observed at 11 epochs in LSTM while the respective figures were 0.05 after 11 epochs and 0.12 after 145 epochs for VGG16. Proposed models exhibited higher degree of accuracy compared to previously reported works. A significant finding of the work was that, data fusion models can further increase diagnosis and prediction performances and build an effective model with larger database. The models would assist the clinicians in prognosis of COVID-19 critical patients effectively in few minutes that will be very helpful to empower the healthcare infrastructure especially in overwhelming healthcare emergency situation as the ongoing COVID pandemic. Early diagnosis could crucially curb viral transmission and facilitate in containing the infection. The authors plan to work on multi-criteria classification as an extended research work to decipher images with mixed lung infections due to several simultaneous infections like tuberculosis, AIDS, COVID-19, etc.

ACKNOWLEDGMENTS

None.

CONFLICT OF INTEREST

The authors declare that there is no conflict of interest.

AUTHORS' CONTRIBUTION

MP and RKM conceptualized the study. MP performed the study. MP, SP and GP analysed and interpreted the data. MP and RKM wrote the original draft. SM, KD wrote, reviewed and edited the manuscript. All authors read and approved the final manuscript for publication.

FUNDING

None.

DATA AVAILABILITY

The datasets generated and/or analysed during the current study are available from the corresponding author on reasonable request.

ETHICS STATEMENT

Not applicable.

REFERENCES

1. Mohapatra RK, Mishra S, Azam M, Dhama K. COVID-19, WHO guidelines, pedagogy, and respite. *Open Medicine.* 2021;16(1):491-493.doi: 10.1515/med-2021-0266
2. Mohapatra RK, Das PK, Pintilie L, Dhama K. Infection capability of SARS-CoV-2 on different surfaces. *Egypt J Basic Appl Sci.* 2021;8(1):75-80.doi: 10.1080/2314808X.2021.1907915
3. Mohapatra RK, Perekhoda L, Azam M, et al. Computational investigations of three main drugs and their comparison with synthesized compounds as potent inhibitors of SARSCoV-2 main protease (Mpro): DFT, QSAR, molecular docking, and *in silico* toxicity analysis. *J King Saud Univ Sci.* 2021;33(2):101315.doi: 10.1016/j.jksus.2020.101315
4. Mohapatra RK, Das PK, Kandi V. Challenges in controlling COVID-19 in migrants in Odisha, India. *Diabetes Metab Syndr.* 2020;14(6):1593-1594.doi: 10.1016/j.dsx.2020.08.024
5. WHO, WHO Coronavirus (COVID-19) Dashboard. 2022. https://covid19.who.int/ (accessed on 02-01-2023)
6. RMohapatra K, Dhama K, El-Arabey AA, et al. Repurposing benzimidazole and benzothiazole derivatives as potential inhibitors of SARS-CoV-2: DFT, QSAR, molecular docking, molecular dynamics simulation, and in-silico pharmacokinetic and toxicity studies. *J King Saud Univ Sci.* 2021;33(8):101637.doi: 10.1016/j.jksus.2021.101637
7. Mohapatra RK, Dhama K, Mishra S. et al. The microbiota related coinfections in COVID-19 patients: a real challenge. *Beni Suef Univ J Basic Appl Sci.* 2021;10(1):47.doi: 10.1186/s43088-021-00134-7
8. McCarthy C, CO'Donnell P, Kelly NEW, O'Shea D, Hogan AE. COVID-19 severity and obesity: are MAIT cells a factor? *Lancet.* 2021;9(5):445-447.doi: 10.1016/S2213-2600(21)00140-5
9. Popkin BM, Du S, Green WD, et al. Individuals with obesity and COVID-19: a global perspective on the epidemiology and biological relationships. *Obes Rev.* 2020;21(11):e13128.doi: 10.1111/obr.13128
10. Lega I, Nistico L, Palmieri L, et al. Psychiatric disorders among hospitalized patients deceased with COVID-19 in Italy. *EClinical Medicine*. 2021;35:100854.doi: 10.1016/j.eclinm.2021.100854
11. Mohapatra RK, Mahal A, Kutikuppala LVS, et al. Renewed global threat by the novel SARS-CoV-2 variants 'XBB, BF.7, BQ.1, BA.2.75, BA.4.6': A discussion. *Front Virol*. 2022;2:1077155.doi: 10.3389/fviro.2022.1077155
12. Jiang X-L, Zhu K-L, Wang X-J, et al. Omicron BQ.1 and BQ.1.1 escape neutralisation by omicron subvariant breakthrough infection. *Lancet Infect Dis.* 2023;23(1):28-30.doi: 10.1016/S1473-3099(22)00805-2
13. Uraki R, Ito M, Furusawa Y, et al. Humoral immune evasion of the omicron subvariants BQ.1.1 and XBB. *Lancet Infect Dis.* 2023;23(1):30-32.doi: 10.1016/S1473-3099(22)00816-7
14. Wang Q, Iketani S, Li Z, et al. Alarming antibody evasion properties of rising SARSCoV-2 BQ and XBB subvariants. *Cell.* 2023;186(2):279-286.doi: 10.1016/j.cell.2022.12.018
15. Pormohammad A, Zarei M, Ghorbani S, et al. Efficacy and Safety of COVID-19 Vaccines: A Systematic Review and Meta-Analysis of Randomized Clinical Trials. *Vaccines*.2021;9(5):467.doi: 10.3390/vaccines9050467
16. Tian F, Yang R, Chen Z. Safety and efficacy of COVID-19 vaccines in children and adolescents: A systematic review of randomized controlled trials. *J Med Virol*. 2022;94(10):4644-4653.doi: 10.1002/jmv.27940
17. Pal M, Parija S, Mohapatra RK, et al. Symptom-Based COVID-19 Prognosis through AI-Based IoT: A Bioinformatics Approach. *BioMed Res Int*. 2022;3113119.doi: 10.1155/2022/3113119
18. Zhang J. Triple-view convolutional neural networks for COVID-19 diagnosis with chest x-ray. 2020. doi: 10.48550/arXiv.2010.14091
19. Haque KF, Abdelgawad A. A deep learning approach to detect COVID-19 patients from chest x-ray images, *Artificial Intelligence.* 2020;3:418-435.doi: 10.3390/ai1030027
20. Ghoshal B, Tucker A. Estimating uncertainty and interpretability in deep learning for coronavirus (COVID-19) detection. Preprint. Posted online March 22, 2020. arXiv:2003.10769. doi: 10.48550/arXiv.2003.10769
21. Islam MZ, Islam MM, Asraf A. A combined deep CNN-LSTM network for the detection of novel coronavirus

(COVID-19) using x-ray images. *Inform Med Unlocked.* 2020;20:100412.doi: 10.1016/j.imu.2020.100412

22. Narin A, Kaya C, Pamuk Z. Automatic detection of coronavirus disease (COVID-19) using x-ray images and deep convolutional neural networks.*Pattern Anal Appl*. 2021;24(3):1207-1220. doi: 10.1007/s10044-021-00984-y
23. Shorfuzzaman M, Masud M, Alhumyani H, Anand D, Singh A. Artificial Neural Network-Based Deep Learning Model for COVID-19 Patient Detection Using X-Ray Chest Images. *J Healthc Eng.* 2021;5513679.doi: 10.1155/2021/5513679
24. COVID Chestxray Dataset. https://github.com/ieee8023/covid-chestxray-dataset (Accessed on December 14, 2022)
25. Yang D, Martinez C, Visuna L, Khandhar H, Bhatt C. Carretero J. Detection and analysis of COVID 19 in medical images using deep learning techniques. *Sci Rep*. 2021;11(1):19638.doi: 10.1038/s41598-021-99015-3
26. Hochreiter S, Schmidhuber J. Long short-term memory. *Neural Comput.* 1997;9(8):1735-1780.doi: 10.1162/neco.1997.9.8.1735
27. Olah C. Understanding LSTM Networks. http://colah.github.io/posts/2015-08- Understanding-LSTMs/ (accessed on 26 June 2018).
28. Apostolopoulos ID, Aznaouridis SI, Tzani MA. Extracting possibly representative COVID-19 biomarkers from X-ray images with deep learning approach and image data related to pulmonary diseases. *J Med Biol Eng.* 2020;40(3):462-469.doi: 10.1007/s40846-020-00529-4
29. Sahinbas K, Catak FO. Transfer learning-based convolutional neural network for COVID-19 detection with X-ray images. Data Science for COVID-19. 2021:451-466.doi: 10.1016/B978-0-12-824536-1.00003-4
30. Guefrechi S, Jabra MB, Ammar A, Koubaa A, Hamam H. Deep learning based detection of COVID-19 from chest X-ray images. *Multimed Tools Appl.* 2021;80(21-23):31803-31820.doi: 10.1007/s11042-021-11192-5
31. Ohata EF, Bezerra GM, Chagas JVS, et al . Automatic detection of COVID-19 infection using chest X-ray images through transfer learning," in IEEE/CAA *Journal of Automatica Sinica*, 2021;8(1): 239-248. doi: 10.1109/JAS.2020.1003393.
32. Joaquin A. Using Deep Learning to Detect Pneumonia Caused by NCOV-19 from X-ray Images. 2020. https://towardsdatascience.com/using-deep-learning-to-detect-ncov-19-from-X-ray-images-1a89701d1acd (accessed on 13 December 2021)
33. Brunese L, Mercaldo F, Reginelli A, Santone A. Explainable deep learning for pulmonary disease and coronavirus COVID-19 detection from X-rays. *Comput Methods Programs Biomed.* 2020;196:105608.doi: 10.1016/j.cmpb.2020.105608
34. Rajaraman S, Antani S. Training deep learning algorithms with weakly labeled pneumonia chest X-ray data for COVID-19 detection. *medRxiv.* 2020.doi: 10.1101/2020.05.04.20090803